Journal of Integrative Agriculture 2026, 25(2): 671–681

Available online at ScienceDirect

Journal of Integrative Agriculture



RESEARCH ARTICLE

The PuMYB93–PuGSTF12 regulatory module promotes anthocyanin accumulation in ‘Nanhong’ pear fruit

Huili Sun[1, 2], Xinyue Wang[2], Qiuping Ren[1], Chunyan Liu[2], Xiaoqian Wang[2#]

[1] *College of Agriculture and Biology, Liaocheng University, Liaocheng 252000, China*
[2] *College of Horticulture, Shenyang Agricultural University, Shenyang 110866, China*

Highlights

- PuMYB93 was identified as a positive regulator of anthocyanin biosynthesis in pear fruit.
- PuMYB93 directly binds to the promoter of the transporter gene *PuGSTF12* to activate its expression, promoting anthocyanin transport and accumulation.
- The PuMYB93–PuGSTF12 regulatory module is essential for red coloration in the ‘Nanhong’ pear mutant.

Abstract

Anthocyanins are important flavonoid pigments in the coloration of fruits. To identify candidate genes involved in anthocyanin accumulation, metabolic and transcriptome analyses were conducted in ‘Nanguo’ pear and its red sport cultivar ‘Nanhong’ pear. The results showed that ‘Nanhong’ pear had significantly higher anthocyanin and flavonol contents. Additionally, transcriptomic analysis showed that there were significant differences in the expression of genes involved in phenylpropanoid and flavonoid biosynthesis pathways between the two cultivars, with *PuGSTF12* being the most upregulated gene in the ‘Nanhong’ cultivar. Further analysis identified a novel MYB transcription factor (PuMYB93), and its silencing repressed *PuGSTF12* expression and anthocyanin accumulation, suggesting it plays an essential role in the regulation of anthocyanin biosynthesis. Moreover, yeast one-hybrid analysis, electrophoretic mobility shift assay, and β-glucuronidase assay indicated that PuMYB93 can directly bind to the *PuGSTF12* promoter to positively regulate its expression. Additionally, *PuGSTF12* silencing suppressed the coloration of *PuMYB93*-OE peels, suggesting that *PuGSTF12* act downstream of PuMYB93. Overall, the findings of this study show that PuMYB93 promotes anthocyanin transport in pears by regulating *PuGSTF12* expression to further enhance anthocyanin accumulation.

Keywords: anthocyanin, pear, transcriptome analysis, transcription factor, PuMYB93

1. Introduction

Over the years, the skin color of pears has been greatly diversified through long-term natural hybridization and human selection (Feng *et al.* 2015). Generally, pear cultivars can be divided into three main types based on their skin color: green, russet, and red (Yang *et al.* 2013). Recently, red pear cultivars have become more popular because of their attractive skin color and potential nutritional value (Wang *et al.* 2020). ‘Nanguo’ is an important pear cultivar (*Pyrus ussuriensis* Maxim.) cultivated in the cold areas of northern China. ‘Nanhong’ is a red-skinned mutant of ‘Nanguo’ pear that appeals to consumers because of its attractive appearance. Anthocyanin accumulation results in red coloration in pear peels. Red skin color is mainly determined by the composition and concentration of anthocyanins (Gao *et al.* 2021); therefore, it is necessary to explore the molecular mechanisms of anthocyanin synthesis in pear fruit and its bud sport mutants.

Anthocyanins are synthesized *via* phenylalanine metabolic pathway through the actions of several catalytic enzymes (Deng and Lu 2017), including phenylalanine ammonia lyase (PAL), chalcone synthase (CHS), chalcone isomerase (CHI), flavanone 3-hydroxylase (F3H), dihydroflavonol 4-reductase (DFR), anthocyanidin synthase (ANS), and

Received 21 October 2024; Received in revised form 28 January 2025; Accepted 29 April 2025; Available online 5 December 2025
[#]Correspondence Xiaoqian Wang, Tel: +86-24-88487219, E-mail: wangxq873@163.com

© 2026 CAAS. Publishing services by Elsevier B.V. on behalf of KeAi Communications Co. Ltd. This is an open access article under the CC BY-NC-ND license (http://creativecommons.org/licenses/by-nc-nd/4.0/). Peer review under responsibility of Editorial Board of *Journal of Integrative Agriculture*.
doi: 10.1016/j.jia.2025.12.002

glycosyltransferase (UFGT). Once anthocyanins are synthesized, they are transported from the cytoplasm to the vacuole for accumulation through the activities of glutathione S-transferase (GST), ATP binding cassette (ABC) proteins, and multidrug and toxic extrusion (MATE) transporters (Zhao and Dixon 2010). *PcGSTF12* has been reported to be involved in anthocyanin and proanthocyanidin accumulation in pears (Zhang *et al.* 2020).

The MYB family of transcription factors (TFs) have been shown to regulate the expression of genes involved in flavonoid biosynthesis (Xu *et al.* 2015). MYB proteins enhance the expression of structural genes by forming MYB-bHLH-WD40 (MBW) complexes with WD-repeat and bHLH (basic helix-loop-helix) proteins, which in turn regulate anthocyanin biosynthesis (Chen *et al.* 2021). Several MYB TFs have been identified and characterized as regulators of flavonoid biosynthesis. In *Arabidopsis*, AtMYB75/PAP1, AtMYB90/PAP2, AtMYB113, and AtMYB114 are involved in regulating anthocyanin biosynthesis (Teng *et al.* 2005). Additionally, several studies have shown that anthocyanin biosynthesis genes are regulated by R2R3-MYB members in pear fruits. For instance, PpMYB10 and PpMYB114, homologs of *Arabidopsis* PAP1 and PAP2, are involved in anthocyanin biosynthesis (Feng *et al.* 2010; Yao *et al.* 2017; Li *et al.* 2025). Moreover, MYB TFs, such as PbMYB10b, PbMYB9, and PpMYB17, regulate anthocyanin biosynthesis by activating anthocyanin-related genes (Zhai *et al.* 2016; Premathilake *et al.* 2020). Recently, another MYB family TF named PbMYB140 was identified as a repressor of anthocyanin accumulation in pears (Ni *et al.* 2021).

Bud mutation is an important method of selecting new red pear varieties. Red mutations are ideal materials used for studying the molecular mechanism of anthocyanin accumulation because of their highly similar genetic backgrounds (Zhang *et al.* 2020). In the present study, our primary goal was to elucidate the molecular and metabolic mechanisms underlying the different pigmentations in the 'Nanguo' pear fruit and its red mutant 'Nanhong'. Metabolic and transcriptome analyses were conducted to elucidate the variations in the colors of the two pear cultivars. Transcription analyses showed that *PuGSTF12* was the most upregulated gene in the 'Nanhong' cultivar and it affected anthocyanin transport. Furthermore, the expression of an MYB gene, *PuMYB93*, correlated with anthocyanin content and *PuGSTF12* expression, suggesting that this gene may be involved in anthocyanin accumulation in pear fruits. The findings of this study provide fresh perspectives and understanding of the colors of 'Nanguo' pear and its mutants 'Nanhong'.

2. Materials and methods

2.1. Plant materials

The experimental materials used for this study were the 'Nanguo' pear and its bud sport variety, the 'Nanhong' pear. These varieties were grafted on the same rootstock and grown in the same orchard in Haicheng, Liaoning, China, and standard horticultural practices were followed in the orchard management. The fruits were collected 140 days after full bloom (DAFB) and immediately transported to the laboratory for sampling and transcriptome data analysis. Fruits bagged in double-layered paper bags were used for candidate *MYB* gene expression analysis. Fruit samples were randomly collected at 0, 1, 4, and 7 d after bag removal. Bagged fruits were sampled simultaneously and used as the control.

Mature fruits of eight pear cultivars, including 'Nanguo', 'Huangguan', 'Xuehua', 'Pingguo', 'Hongxiangsu', 'Zaosu', 'Hongzaosu', and 'Nanhong', were used for *PuMYB93* expression analysis. Moreover, transient expression validation tests were performed using ripe bagged 'Pingguo' pear (*Pyrus bretschneideri*) fruits. Three biological replicates were used for each sample. All fruits were peeled, immediately frozen in liquid nitrogen, and stored at –80°C for subsequent experiments.

Pear calli were induced from the 'Nanguo' pear flesh and were used for the GUS assay. The calli were grown on MS medium containing 2.0 mg L^{-1} 2,4-dichlorophenoxyacetic acid (2,4-D) and 1.5 mg L^{-1} 6-BA and at 25°C in the dark.

2.2. Phenolic extraction and analysis

Phenolic compounds were extracted according to the method described by Wang *et al.* (2015). Briefly, frozen peel samples weighting 0.5 g were firstly grinded with liquid nitrogen, and then extracted with 10 mL of 70% methanol containing 2% formic acid. After being shaken in a thermomixer at 30°C for 30 min at 1,000 r min^{-1}, this combined homogenate was centrifuged at 10,000 g for 10 min. The supernatant was then filtered through a 0.45-μm syringe filter prior to subsequent analysis.

The phenolic compounds were determined using an ACQUITY UPLC H-Class Waters instrument (Waters, Milford, MA, USA) coupled to a XEVO TQD mass spectrometer (Waters, Milford, MA, USA). Samples were separated on a BEH C18 column (2.1 mm×50 mm, 1.7 mm) (Waters, Milford, MA, USA) with the following settings: column temperature, 45°C, flow rate, 0.35 mL min^{-1}, and injection volume, 10 μL. Mobile phase A was distilled water containing 0.1% formic acid, and B was methanol. The gradient conditions were: 0 min, 2% B, 10 min, 30% B, and 12 min, 95% B. The capillary voltage of Waters XEVO TQD was set to 2.5 kV. The source temperature was set at 150°C and desolvation gas temperature at 500°C to a flow of 1,000 L h^{-1}. The data was analyzed by Masslynx software (Waters).

2.3. RNA extraction and transcriptome sequencing

The peels of 'Nanhong' and 'Nanguo' fruits were used for transcriptome analysis. Total RNA was extracted from each sample by the CTAB method, using Sangon Total RNA Purification Kit (Sangon Biotech, Shanghai, China). RNA sequencing and assembly were conducted by Biomarker Technologies Corporation (Beijing, China). Library construction and sequencing were performed using Illumina HiSeq 2500 platform (Illumina, CA, USA). Differential expression analysis was performed using DESeq2, and cluster profiles with $P \leq 0.01$ and fold change≥2 were considered differentially expressed genes (DEGs). Gene Ontology (GO) and Kyoto Encyclopedia of Genes and

Genomes (KEGG) enrichment analyses of DEGs were performed using the GOseq R language package and the KEGG pathway database, respectively (Young *et al.* 2010).

2.4. Gene expression profiles

First-strand cDNA synthesis was performed using a PrimeScript RT Reagent Kit, and qRT-PCR was performed using a SYBR Green kit (Takara, Tokyo, Japan) on a 7500 real-time PCR system (Applied Biosystems, Foster City, CA). *PuActin* served as the internal control. The primers used for qRT-PCR are listed in Appendix A.

2.5. Subcellular localization

Vector construction and experimental procedures for determining the subcellular localization of PuMYB93 were performed, according to the methods described by Wang *et al.* (2021). The coding region of *PuMYB93* was fused in frame to the N-terminus of green fluorescent protein (GFP) to form the fusion vector *35S-PuMYB93-GFP*, which was then transiently expressed in tobacco leaves by Agrobacterium infiltration (GV3101). The GFP florescence of the transiently infected leaves was measured by a TCS SP8 confocal microscope (Leica, Germany).

2.6. Transient transformation analysis in pear fruit

The full-length coding sequence (CDS) of *PuMYB93* gene was independently cloned into *pCAMBIA1301S* vector containing *CaMV35S* promoter and *GFP* gene, resulting in a fusion gene driven by 35S promoter. A 300 bp fragment within the *PuMYB93 and PuGSTF12* gene was forward and reverse amplified and cloned into the *pFGC5941* vector to construct a silent fusion vector. Mature bagged 'Pingguo' pear fruits were used for the transient expression assay. The fruits were infiltrated with transformed *Agrobacterium* cells using needleless syringes, stored overnight in the dark and then under continuous white light provided by overhead LEDs in a light incubator for 5 d (day/night=16 h/8 h, temperature 20°C, and relative humidity 70%). Peels from the injection periphery was collected for anthocyanin extraction and gene expression analysis.

2.7. β-Glucuronidase (GUS) assay

The promoters of *PuANS*, *PuUFGT* and *PuGSTF12* were fused to the transformed *pBI101-GUS* vector to activate the *GUS* reporter gene. The primers are listed in Appendix B. *Agrobacterium tumefaciens* strain GV3101 containing the vector was independently infiltrated into the *PuMYB93*-OE pear calli. The transgenic calli carrying the empty vector were used as the control. Histochemical GUS staining was performed as per He *et al.* (2012). GUS activity was measured as per Jefferson *et al.* (1987).

2.8. Yeast one-hybrid (Y1H) assay

The CDS of *PuMYB93* and the cloned promoter of *PuGSTF12* were ligated into the pGADT7 and pAbAi vectors, respectively, and Y1H assays were performed as described by Li *et al.* (2016). All the primers used are listed in Appendix B.

2.9. Electrophoretic mobility shift assay (EMSA)

EMSA was performed using the LightShift Chemiluminescent EMSA Kit as previously described (Li *et al.* 2016). Oligonucleotide probes were synthesized and labeled with biotin. The biotin-labeled *PuGSTF12* promoter sequences were as shown in Appendix B. For the EMSA assay, recombinant His-tagged PuMYB93 were expressed in *E. coli* BL21 and purified using nuclear protein and cytoplasmic protein extraction kit (Beyotime, Shanghai, China).

2.10. Data analysis

All data were analyzed using SPSS 17.0. Student's two-tailed *t*-test ($P<0.05$) was used to determine differences between the two groups. Phylogenetic analysis was conducted using MEGA 5.0. Transcriptome data statistics and some figures were prepared on biomarker cloud platform (Biomarker Biotechnology Co., Bingjing, China).

3. Results

3.1. Phenolic profiles of 'Nanguo' and 'Nanhong' pear fruit peels

The phenotypes of mature fruits of 'Nanguo' and its red mutant 'Nanhong' are presented in Fig. 1-A. The phenolic profiles of the cultivars were determined by ultra-high performance liquid chromatography-mass spectrometry (UPLC-MS) (Appendix C). A total of four flavanols were detected, including two monomers (catechin and epicatechin) and two dimers (procyanidins B1 and B2). Additionally, the 'Nanhong' cultivar had significantly lower flavanol content than the 'Nanguo' cultivar. Moreover, the flavonol metabolites included four types of quercetin and three types of isorhamnetin glycosides, and the anthocyanins included cyanidin and peonidin glycosides. Furthermore, the flavonol and anthocyanin contents of 'Nanhong' fruits were significantly higher than those of 'Nanguo' fruits (Fig. 1-B). In particular, the contents of anthocyanins in 'Nanhong' (58.76 mg kg^{-1}) were significantly higher than those in 'Nanguo' (1.67 mg kg^{-1}), indicating the differential metabolism of anthocyanin in the two cultivars.

3.2. Transcriptome analysis

Transcriptome analysis was performed on 'Nanguo' (control) and 'Nanhong' to elucidate the mechanism of anthocyanin biosynthesis (Appendix D). Differential expression analysis identified a total 507 DEGs between the two cultivars, among which 275 were upregulated and 232 were downregulated (Fig. 2-A). Gene ontology analysis showed that the 507 DEGs were enriched in 36 functional terms belonging to biological process, cellular component, and molecular function categories (Fig. 2-B). Additionally, KEGG pathway analysis showed that the top 20 enriched pathways included biosynthesis of secondary metabolites, such as phenylpropanoid biosynthesis and flavonoid biosynthesis (Fig. 2-C). Notably, 12 DEGs were enriched in phenylpropanoid biosynthesis, making it the dominant pathway.

3.3. DEGs related to anthocyanin synthesis and transport

KEGG enrichment analysis of the DEGs showed that four

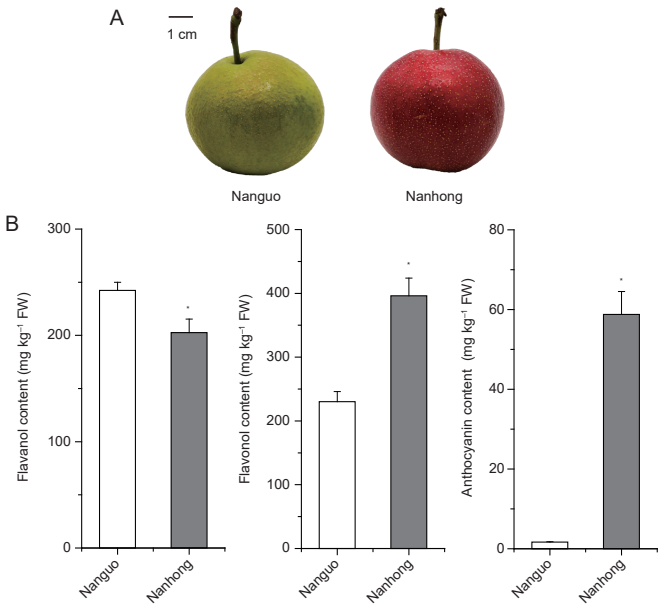


Fig. 1 Visual appearances and flavonoid contents of the 'Nanguo' and 'Nanhong' fruits. A, two pear cultivars with different peel colors. B, contents of flavanols, flavonols and anthocyanins in peel of two pear cultivars. Error bars: standard deviations (three replications). *, $P<0.05$.

UFGT genes were significantly upregulated in 'Nanhong' than in 'Nanguo' (Fig. 3). However, no significant differences were found in the expression levels of other structural genes involved in anthocyanin biosynthetic pathway. Studies have shown that anthocyanins are synthesized in the cytoplasm and transported to the vacuole for accumulation (Gomez *et al.* 2009; Sun *et al.* 2012; Francisco *et al.* 2013). A total of seven putative genes encoding proteins involved in anthocyanin transport, including three *GST* genes, three *ABC* genes, and one *MATE*, were identified. Additionally, the expression profiles of the seven genes were significantly higher in the 'Nanhong' cultivar than those in the 'Nanguo' cultivar, among which one *GST* transporter gene (*PuGSTF12*, LOC103959931) was upregulated by 167.67-fold in the 'Nanhong' cultivar when compared with that in the 'Nanguo' cultivar. These results suggest that *PuGSTF12* is the most likely transport gene involved in anthocyanin accumulation.

3.4. qPCR analysis of candidate MYBs related to anthocyanin accumulation

The TFs are able to regulate the expression of anthocyanin biosynthesis-related genes, and we identified 33 TFs among the DEGs (Appendix D). The most enriched TFs included MYB, ERF, bHLH, and WRKY, among which *MYB* genes were the most important involved in secondary metabolism. Among the DEGs, nine members of the *MYB* family were filtered, among which six were upregulated (Fig. 3). The *MYB* family members included *PuMYB110a* (*LOC103959467*), which is highly homologous to *PpMYB10* (*Pbr016661.1*), and *PuMYB114* (*LOC103952399*), which encodes a homolog of *PpMYB114* (*Pbr042132.1*). To identify candidate MYB TFs responsible for pigmentation in 'Nanhong', the expression profiles of TFs were investigated by qRT-PCR during light exposure stages in 'Nanhong' peel (Fig. 4). After bag removal, the fruits gradually began to turn red and accumulated considerably higher levels of anthocyanins. Additionally, there was a rapid increase in the expression levels of and transporter gene (*PuGSTF12*) and regulator genes (*PuMYB110a* and *PuMYB114*), which peaked 1 d after bag removal prior to anthocyanin accumulation. Compared with the control group (bagged fruits), the peel of debagged fruits exhibited lower expression levels of *LOC103929184*, *LOC103938767*, and *LOC103947165*, 4 d after bag removal, indicating that the genes do not participate in the regulation of anthocyanin biosynthesis in pears. However, exposed peels had higher expression levels of *LOC103930480* than that of the bagged peels, with similar expression trends as *PuMYB110a* and *PuGSTF12*. This result indicated that *LOC103930480* may be involved in the regulation of anthocyanin biosynthesis in 'Nanhong' peel.

3.5. Expression pattern of *PuMYB93*

Phylogenetic analysis was performed to determine the evolutionary relationship between *LOC103930480* and other known R2R3-MYB anthocyanin regulating genes in *Malus* and *Arabidopsis* (Teng *et al.* 2005; Chen *et al.* 2021). The results showed that it was clustered into subgroup C2, homologous to *MdMYB93 (MDP0000320772)* and *AtMYB93* (*AT1G12630.1*); therefore, it was designated as *PuMYB93* (Fig. 5-A). The 2,000-bp upstream sequence of *PuMYB93* was analyzed using tools at the PlantCARE (Appendix E). Regarding tissue specificity, *PuMYB93* was predominantly expressed in the roots, stems, and peels of 'Nanhong' plants (Fig. 5-B). Subcellular localization analysis revealed that PuMYB93 was localized in the nucleus (Fig. 5-C). Additionally, correlation analysis between anthocyanin content and *PuMYB93* expression using the peel of mature fruits from eight pear cultivars showed that *PuMYB93* expression was positively correlated with anthocyanin content (Fig. 5-D). Particularly, *PuMYB93* expression levels were higher in red pear cultivars than the other cultivars. These results suggest that *PuMYB93* is involved in anthocyanin accumulation.

3.6. *PuMYB93* silencing influences pear fruit coloration

To investigate whether PuMYB93 is essential for anthocyanin accumulation, transient expression analyses was conducted using *PuMYB93*-RNAi. A partial CDS of *PuMYB93* gene was similarly ligated into the *pFGC5941* vector to generate a silent fusion vector, which was transiently infiltrated into bagged pear fruits. Compared with fruits injected with the control vector, the site of fruits injected with the silenced vector remained pale after being illuminated (Fig. 6-A and B). Additionally, silencing *PuMYB93* significantly reduced the expression of *PuANS*, *PuUFGT*, and *PuGSTF12* (Fig. 6-C and D). Overall, these results showed that the silencing of *PuMYB93* affected anthocyanin biosynthesis in pear fruit.

3.7. PuMYB93 activates *PuGSTF12*

To investigate the mechanism through which PuMYB93

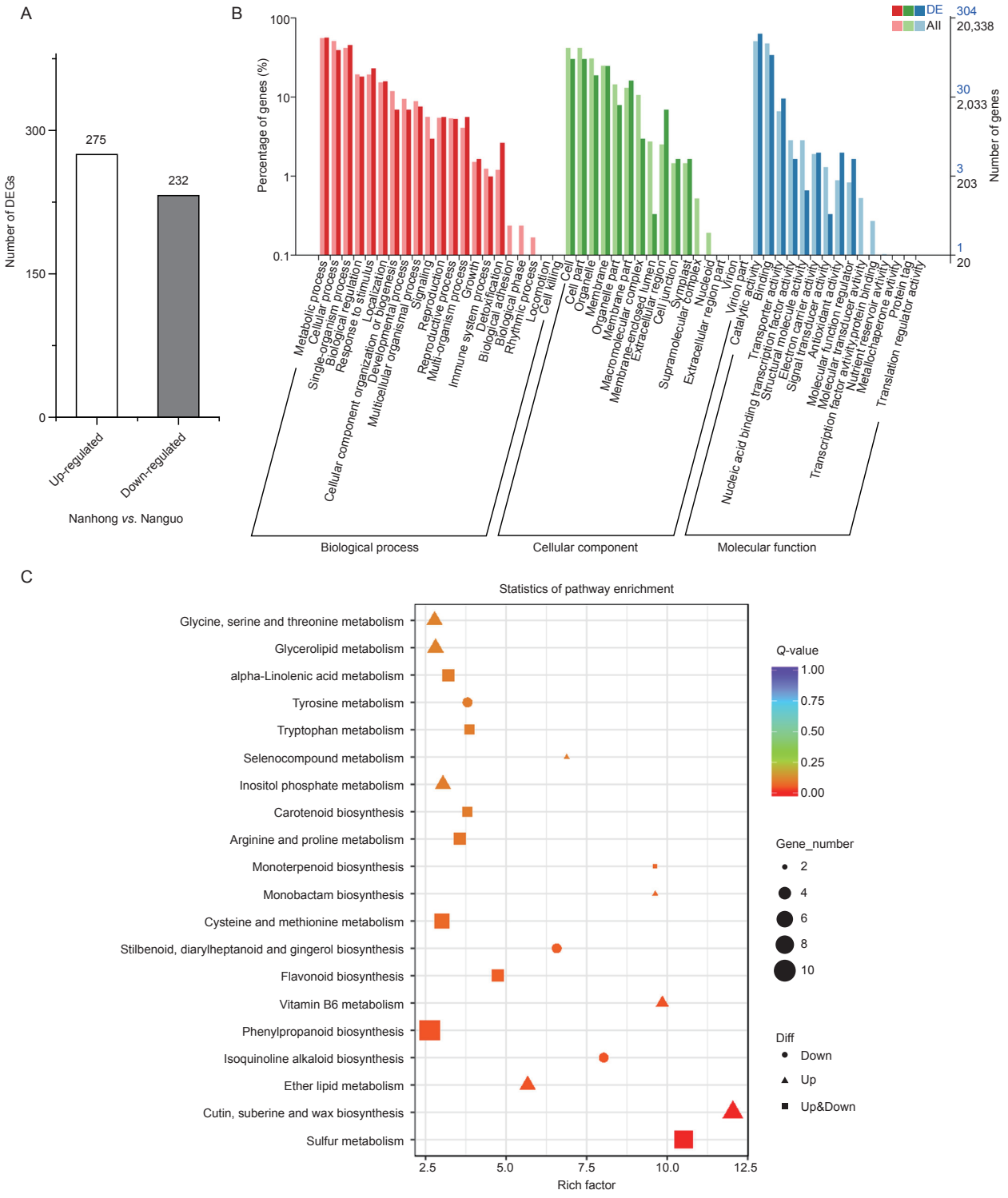


Fig. 2 The number and general bioinformatics analysis of differentially expressed genes (DEGs). A, numbers of DEGs between 'Nanguo' and 'Nanhong' fruits. B, gene ontology (GO) classifications of the annotated unigenes. C, Kyoto Encyclopedia of Genes and Genomes (KEGG) enrichment analyses of DEGs.

regulates anthocyanin accumulation, a Y1H assay was performed using the PuMYB93-pGADT7 and *PuGSTF12*-pAbAi vectors. The Y1H assay showed that PuMYB93 binds to *PuGSTF12* promoter (Fig. 7-A). To confirm this result, an EMSA was further conducted and a MYB-core type element within an 1,107-bp region upstream of the start codon was found in the *PuGSTF12* promoter. The results showed that PuMYB93 could interact with DNA probes containing this MYB-binding sites (TAACCA) (Fig. 7-B). Furthermore, the GUS assay showed that PuMYB93 directly activated *PuGSTF12* (Fig. 7-C). Therefore, it could be concluded that PuMYB93 binds directly to *PuGSTF12* and positively

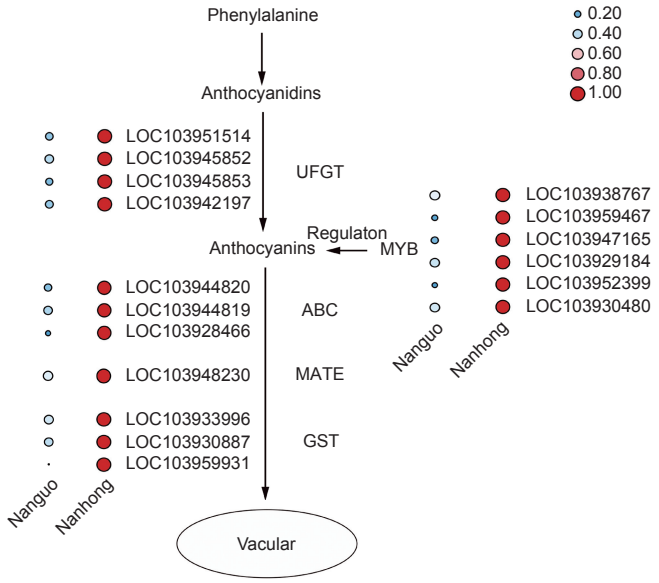


Fig. 3 Heat map diagram of the relative expression levels of anthocyanin biosynthesis-related genes. The expression level of genes is indicated using filled circles of different sizes and colors. The larger the circle, the higher the expression.

regulates its activity. We also investigated the role of PuMYB93 in the regulation of *PuANS* and *PuUFGT* promoter in pear calli using a GUS assay. The results revealed that PuMYB93 could not increase *PuANS* and *PuUFGT* promoter activity (Appendix F).

3.8. PuMYB93 functions upstream of *PuGSTF12*

Given that PuMYB93 directly binds the *PuGSTF12* promoter, and *PuGSTF12* was reduced in *PuMYB93*-RNAi peels, we hypothesized that *PuGSTF12* is a direct downstream target of PuMYB93. To test this hypothesis, we crossed the 35S-*PuMYB93*-GFP construct into the *PuGSTF12*-RNAi peels. The results clearly showed that the silencing of *PuGSTF12* significantly suppressed the coloration of *PuMYB93*-OE peels (Fig. 8-A). The anthocyanin contents of *PuMYB93*-OE peels was largely reduced in the *PuGSTF12*-RNAi background (Fig. 8-B). qRT-PCR analysis showed that the expression of *PuMYB93* in the *PuMYB93*-OE/*PuGSTF12*-RNAi peels were indeed markedly upregulated. Additionally, the expression of *PuGSTF12* and *PuUFGT* was significantly increased in the *PuMYB93*-OE peels. However, after silencing of *PuGSTF12*, *PuMYB93*-OE peels showed significantly lower expression of *PuANS* and *PuUFGT* compared to before silencing (Fig. 8-C). These results suggest that *PuGSTF12* act downstream of PuMYB93, and the coloration of *PuMYB93*-OE peels is partially dependent on the PuMYB93 promoted transcription of *PuGSTF12*.

4. Discussion

Fruit peel color is an important visible parameter of fruit quality and plays an important role in consumer appeal (Yang *et al.* 2013; Ding *et al*. 2025). Previous studies have shown that red skin pear color is caused by the accumulation of anthocyanins. Similarly, the present study demonstrated that the peels of ‘Nanhong’ pear exhibited higher anthocyanin and flavonol contents than that of ‘Nanguo’ pear, which is in agreement with findings in green ‘Anjou’ pear and its red bud mutation (Li *et al.* 2014). These results suggest that anthocyanin content causes differences in pigmentation between green- and red-peeled pears. Additionally, transcriptomic analysis identified a total of 275 upregulated and 235 downregulated DEGs between ‘Nanguo’ and ‘Nanhong’ pear varieties, which were annotated in GO and KEGG databases. Among the enriched KEGG pathways, phenylpropanoid biosynthesis and flavonoid biosynthesis, were related to anthocyanin biosynthesis, and the upregulation of these pathways contributes to increase in anthocyanin content in ‘Nanhong’ peel.

The anthocyanin biosynthetic pathway has been extensively studied in many plants, and most genes in pear have been isolated (Fischer *et al.* 2007). In the present study, transcriptome analysis showed that among anthocyanin biosynthesis genes, only *UFGT* genes were significantly upregulated in ‘Nanhong’ when compared with ‘Nanguo’. Similar results were recently reported by Liu *et al.* (2023), who found that, except for *UFGT*, most structural genes of the anthocyanin synthesis pathway were not associated with the anthocyanin accumulation patterns in ‘Nanguo’ and ‘Nanhong’ at the different stages of fruit development. Thus, UFGT, as the final enzyme in the anthocyanin synthesis pathway, may play more significant role in anthocyanin biosynthesis in red pear peels.

Anthocyanins are synthesized in the cytoplasm and transported into acidic vacuoles, which gives the plants a rich color (Liu *et al.* 2019a). Previous studies have shown that anthocyanin transporter GSTs play critical roles in anthocyanin accumulation, such as *FvRAP* in strawberry (Luo *et al.* 2018), *MdGSTF6* in apple (Jiang *et al.* 2019), *AcGST1* in kiwifruit (Liu *et al.* 2019b), and *PpGST1* in peach (Zhao *et al.* 2020). Zhang *et al.* (2020) confirmed that *PcGSTF12* gene is transcriptionally related to both anthocyanin and proanthocyanidin biosynthesis in pear. Similarly, the findings of the present study showed that *PuGSTF12* was significantly upregulated in ‘Nanhong’ pear compared to that in the green-peeled ‘Nanguo’ pear, indicating that *PuGSTF12* may be involved in anthocyanin transport in ‘Nanhong’ plants.

The R2R3-MYB TF regulates anthocyanin accumulation in Rosaceae plants mainly by modulating the expression of structural genes involved in the anthocyanin biosynthetic pathway (Wang *et al*. 2010). In ‘Nanhong’ pears, *PuMYB110a* was highly expressed and could positively regulate the transcription of *PuUFGT* and *PuGSTF6*, finally leading to anthocyanin accumulation (Liu *et al.* 2023). Similarly, three highly upregulated *MYB* genes were identified in the red skinned samples in the present study, including *PuMYB110a* and *PuMYB114*. However, phylogenetic analysis of a putative gene identified in the present study against *Arabidopsis* R2R3-MYBs identified another R2R3-MYB protein, PuMYB93. Further analysis showed that the expression of *PuMYB93* is similar to those of *PuMYB110a* and *PuGSTF12* during the light exposure stages in ‘Nanhong’ peel. *AtMYB93* is specifically expressed in root endodermal cells in *Arabidopsis* and negatively regulates lateral root development (Gibbs *et al.* 2014). In apple fruit

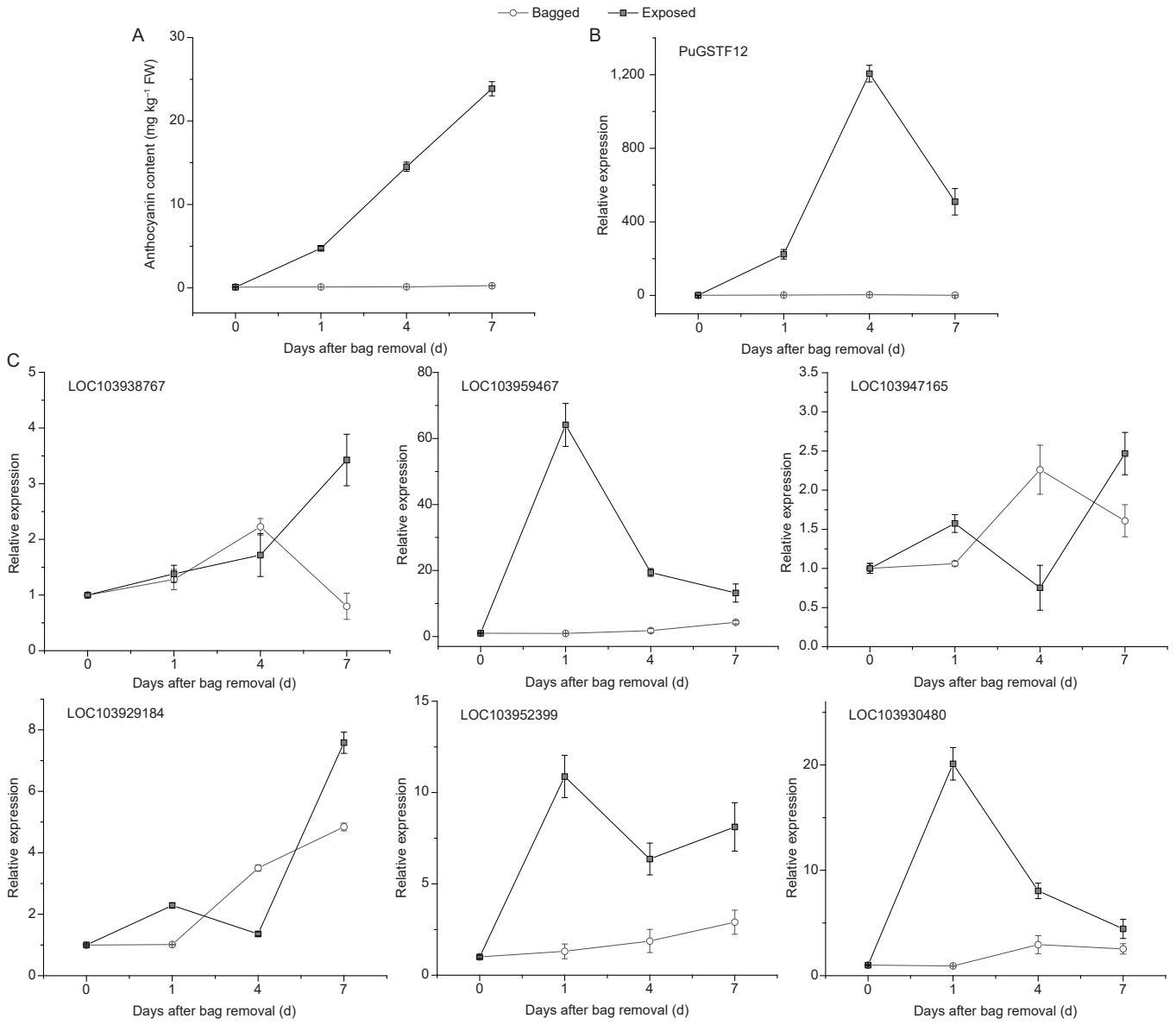


Fig. 4 Anthocyanin contents and transcript levels of candidate genes in peel from 'Nanhong' fruits at 0, 1, 4, and 7 d after bag removal. A, changes in total anthocyanin content in the peel. B and C, expression analysis of *PuGSTF12* (B) and candidate *MYB* genes (C) related to anthocyanin biosynthesis using qRT-PCR. Error bars: standard deviations (three replications).

skin, MdMYB93 has been identified as a regulator of suberin deposition (Legay *et al.* 2016). Gene expression profiling of *MdMYB93* agro-infiltrated leaves revealed concomitant alterations in lipid and phenylpropanoid metabolism, suberin deposition, and extracellular transport. However, *MYB93* is yet to be implicated in anthocyanin biosynthesis.

In the present study, there was a significant increase in *PuMYB93* expression in exposed peels compared with bagged peels. Tissue specificity analysis showed that *PuMYB93* was predominantly expressed in the roots, stems, and peels. Additionally, there was a positive correlation between *PuMYB93* expression levels and the anthocyanin content of the peels of different pear cultivars. Therefore, we speculated that PuMYB93 may be involved in anthocyanin accumulation in pear fruits. Moreover, transient expression validation experiments in pear peels showed that *PuMYB93* silencing repressed anthocyanin accumulation. These findings suggested that PuMYB93 plays an essential role in the regulation of anthocyanin biosynthesis.

In pears, MYB114 can bind to the promoters of *ANS*, *UFGT*, and *GSTF12* to regulate anthocyanin synthesis (Yao *et al.* 2017; Zhang *et al.* 2020). Similarly, the results of the present study showed that *PuMYB93* overexpression or silencing altered the expression of *PuGSTF12* in the fruits. Additionally, Y1H, EMSA and GUS assays showed that PuMYB93 interacted with the promoter *PuGSTF12*, enhancing its activity. Moreover, several studies have suggested that *GSTs* are regulated by MYBs. For instance, *MdGSTF6* is directly regulated by MdMYB1 in apples (Jiang *et al.* 2019). Additionally, PpMYB10.1 binds to the promoter *PpGST1* and activates its transcription in peach (Zhao *et al.* 2020). The present study demonstrated that PuMYB93

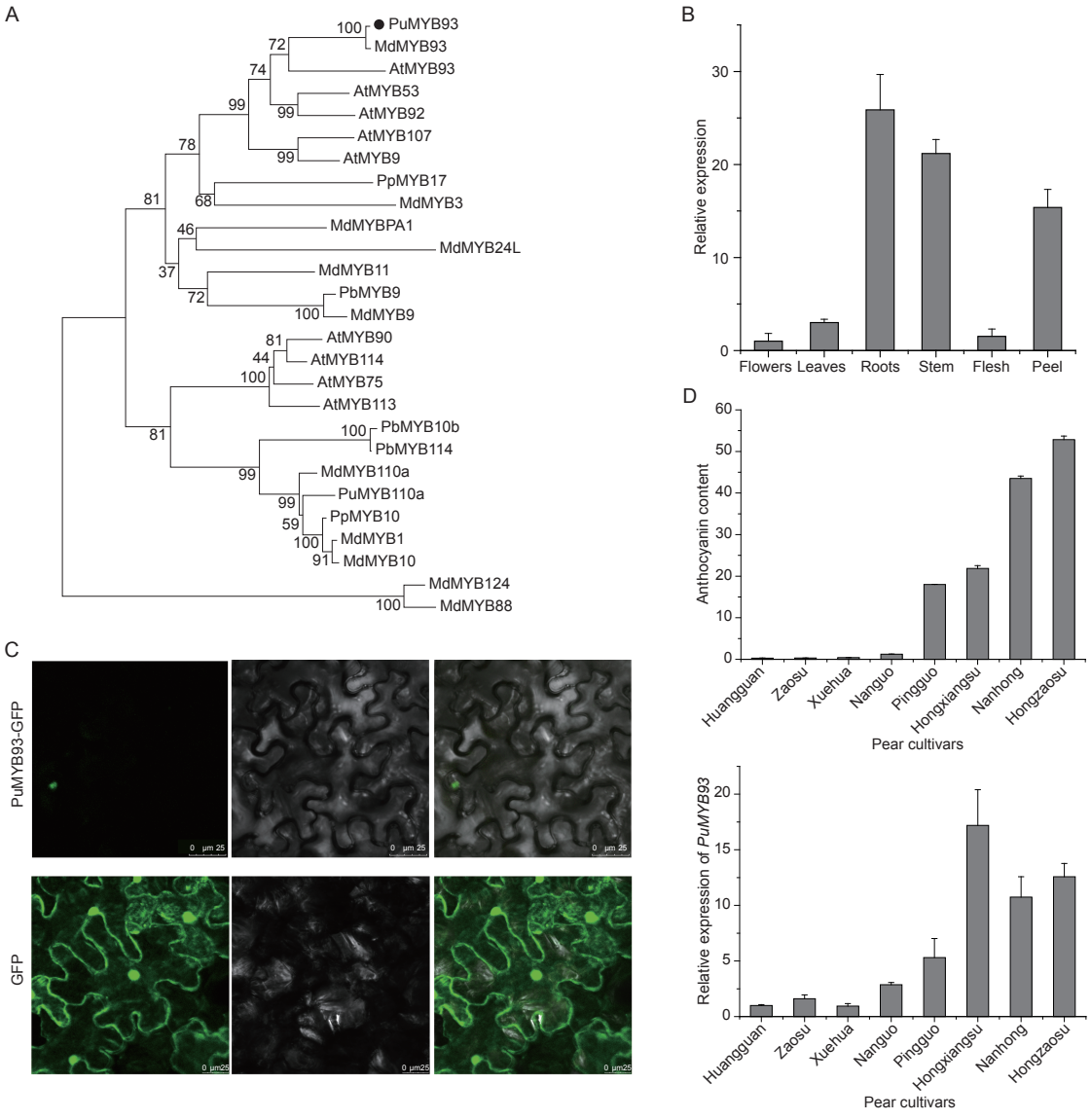


Fig. 5 Phylogenetic analysis and relative expression levels of *PuMYB93*. A, phylogenetic relationships among PuMYB93 and other known anthocyanin-regulating MYB transcription factors in *Malus* and *Arabidopsis*. B, *PuMYB93* expression in various tissues. C, subcellular localization analysis of PuMYB93. D, anthocyanin content and relative expression of *PuMYB93* in the peel of fully ripe fruit among eight pear cultivars. Error bars: standard deviations (three replications).

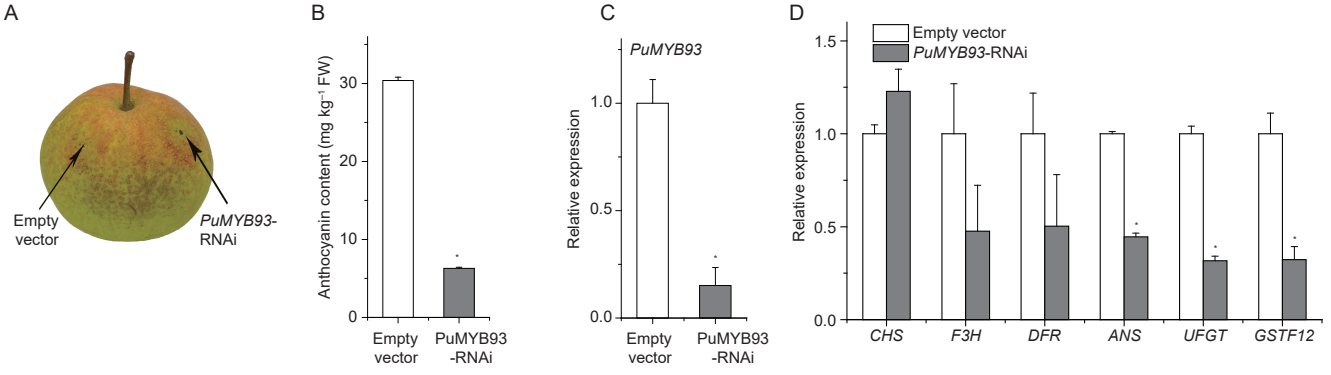


Fig. 6 Effects of *PuMYB93* silencing in bagged 'Pingguo' pear fruit. A, phenotypes of 'Pingguo' fruits after silencing *PuMYB93*. B–D, anthocyanin contents (B), transcript analysis of *PuMYB93* (C) and anthocyanin related genes (D) in *PuMYB93*-silenced fruits and control. An empty vector was used as the control. Error bars: standard deviations (three replications). *, $P<0.05$.

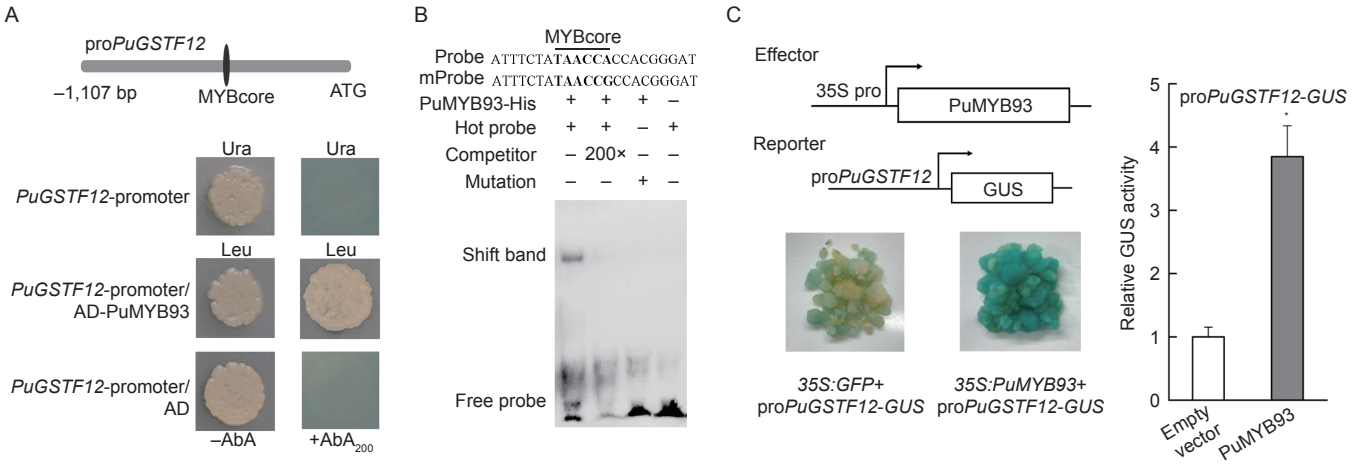


Fig. 7 Analyses of the interaction between PuMYB93 and the *PuGSTF12* promoter. A, yeast one-hybrid assays showing the interaction between PuMYB93 and the *PuGSTF12* promoter. B, electrophoretic mobility shift assay showing that PuMYB93 directly binds the *PuGSTF12* promoter. C, validation of the activation of the *PuGSTF12* promoters by PuMYB93 based on a β-glucuronidase assay activity assay in pear calli. An empty vector was used as the control. Error bars: standard deviations (three replications). *, $P<0.05$.

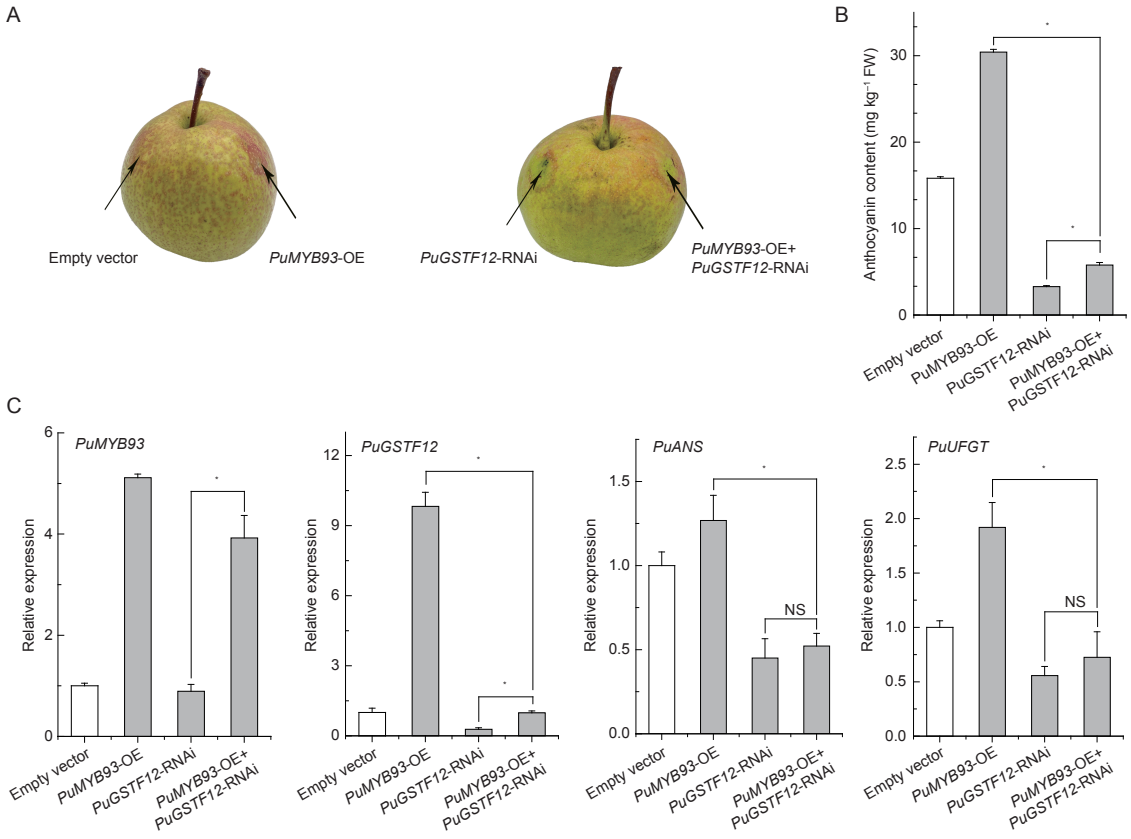


Fig. 8 Silencing of *PuGSTF12* suppressed the coloration of *PuMYB93*-OE peels. A, phenotypes of *PuMYB93*-OE peels after silencing of *PuGSTF12*. B and C, anthocyanin contents (B) and transcript analysis of *PuMYB93* and anthocyanin biosynthesis-related genes (*PuGSTF12*, *PuANS* and *PuUFGT)* (C) in fruit peels around the injection sites. An empty vector was used as the control. Error bars: standard deviations (three replications). *, $P<0.05$. NS, not significant.

regulates *PuGSTF12* in pear fruit. Similarly, there was an increase in the expression of several phenolic metabolism genes and transmembrane transporters in tobacco leaves overexpressing *MdMYB93*, suggesting a potential link between MYB93 and phenylpropanoid metabolism and their transporters (Legay *et al.* 2016).

Except for *PuGSTF12*, overexpression or silencing of *PuMYB93* could also affect the expression of anthocyanin biosynthesis-related genes (*PuANS* and *PuUFGT*). However, PuMYB93 cannot increase *PuANS* and *PuUFGT* promoter activity directly. Further transient expression analysis revealed that *PuMYB93*-OE peels showed significantly lower expression

of *PuANS* and *PuUFGT* after silencing of *PuGSTF12* than before slilencing, indicating that the silencing of *PuGSTF12* inhibited the response of anthocyanin biosynthetic genes to show overexpression of *PuMYB93* in pear peels. Consistent with this result, *MdGSTU12* overexpression promoted the expression of anthocyanin biosynthesis-related genes in transgenic calli and apple fruits (Zhao *et al.* 2021). This may be due to the negative feedback regulation induced by *GST* overexpression, which stimulated the expression of upstream synthesis-related genes to produce more anthocyanins and ultimately promote the accumulation of anthocyanin. Shao *et al.* (2021) corroborated these findings by reporting that the overexpression of *GhGSTF12* accelerated anthocyanin accumulation in cotton leaf. Additionally, genes involved in anthocyanin biosynthesis, regulation, and transport were considerably affected by *PcGSTF12* gene, suggesting that it may not only be a transporter of anthocyanins, but may also be involved in several other steps of anthocyanin accumulation (Zhang *et al.* 2020). Thus, this result obtained showed that PuMYB93 functions in anthocyanin transport in pears by regulating PuGSTF12 activity, which further affects anthocyanin accumulation.

5. Conclusion

In this study, a combined metabolome and transcriptome approach was used to compare the anthocyanin content and biosynthetic pathways in the peels of green 'Nanguo' pear and its red mutant 'Nanhong' pear. The results showed that most DEGs were associated with secondary metabolites, such as phenylpropanoids and flavonoids. Among the DEGs, seven genes involved in anthocyanin transport were identified, with *PuGSTF12* being the most upregulated gene in the red-peeled 'Nanhong'. Additionally, a novel MYB TF, PuMYB93, was shown to promote anthocyanin accumulation in a transient transformation assay. Further analysis revealed that PuMYB93 promotes the expression of *PuGSTF12* by activating its promoter, thereby inducing anthocyanin accumulation in pears. Overall, the findings of the present study contributes to the understanding of the molecular mechanisms of anthocyanin biosynthesis in pear, which could facilitate breeding pears of desirable peel color.

Acknowledgements

The research was supported by the National Natural Science Foundation of China (32372641), the Shandong Provincial Natural Science Foundation, China (ZR2024QC143) and the Liaoning Provincial Natural Science Foundation, China (2022-MS-258).

Declaration of competing interest

The authors declare that they have no conflict of interest.

Declaration of generative AI and AI-assisted technologies in the writing process

The authors declare that they did not use AI in the preparation and writing of this manuscript.

Appendices associated with this paper are available at https://doi.org/10.1016/j.jia.2025.12.002

References

Chen Z, Yu L, Liu W, Zhang J, Wang N, Chen X. 2021. Research progress of fruit color development in apple (*Malus domestica* Borkh.). *Plant Physiology and Biochemistry*, **162**, 267–279.

Deng Y X, Lu S F. 2017. Biosynthesis and regulation of phenylpropanoids in plants. *Critical Reviews in Plant Sciences*, **36**, 257–290.

Ding T, Ma X, Yu X, Wang L, Zhou R, Hou X, Zhao Y. 2025. Integrated transcriptomic and metabolomic analyses reveal the mechanisms for red fruit coloration in peach cv. 'Zhongyoupan 9' under artificial darkness. *Journal of Integrative Agriculture*, **24**, 3866–3879.

Feng S, Wang Y, Yang S, Xu Y, Chen X. 2010. Anthocyanin biosynthesis in pears is regulated by a R2R3-MYB transcription factor PyMYB10. *Planta*, **232**, 245–255.

Feng S Q, Sun S S, Chen X L, Wu S J, Wang D Y, Chen X S. 2015. PyMYB10 and PyMYB10.1 interact with bHLH to enhance anthocyanin accumulation in pears. *PLoS ONE*, **10**, e0142112.

Fischer T C, Gosch C, PfeiVer J, Halbwirth H, Halle C, Stich K, Forkmann G. 2007. Flavonoid genes of pear (*Pyrus communis*). *Trees*, **21**, 521–529.

Francisco R M, Regalado A, Ageorges A, Burla B J, Bassin B J, Eisenach C, Zarrouk O, Vialet S, Marlin T, Chaves M M, Martinoia E, Nagya R. 2013. ABCC1, an ATP binding cassette protein from grape berry, transports anthocyanidin 3-*O*-Glucosides. *The Plant Cell*, **25**, 1840–1854.

Gao H N, Jiang H, Cui J Y, You C X, Li Y Y. 2021 The effects of hormones and environmental factors on anthocyanin biosynthesis in apple. *Plant Science*, **312**, 111024.

Gibbs D J, Voß U, Harding S, Fannon J, Moody, A, Yamada E, Swarup K, Nibau C, Bassel G, Choudhary A, Lavenus J, Bradshaw S, Stekel D, Bennett M, Coates J. 2014. *AtMYB93* is a novel negative regulator of lateral root development in Arabidopsis. *New Phytologist*, **203**, 1194–1207.

Gomez C, Terrier N, Torregrosa L, Vialet S, Level A, Verries C, Souquet J M, Mazauric J P, Klein M, Cheynier V, Ageorges A. 2009. Grapevine MATE-type proteins act as vacuolar H^+-dependent acylated anthocyanin transporters. *Plant Physiology*, **150**, 402–415.

He J, Duan Y, Hua D, Fan G, Wang L, Liu Y, Chen Z, Han L, Qu L, Gong Z. 2012. DEXH box RNA helicase-mediated mitochondrial reactive oxygen species production in Arabidopsis mediates crosstalk between abscisic acid and auxin signaling. *The Plant Cell*, **24**, 1815–1833.

Jefferson R A, Kavanagh T A, Bevan M W. 1987. GUS fusions: Beta-glucuronidase as a sensitive and versatile gene fusion marker in higher plants. *The Embo Journal*, **6**, 3901–3907.

Jiang S, Chen M, He N, Chen X, Wang N, Sun Q, Zhang T, Xu H, Fang H, Wang Y, Zhang Z Y, Wu S J, Chen X S. 2019. MdGSTF6, activated by MdMYB1, plays an essential role in anthocyanin accumulation in apple. *Horticulture Research*, **6**, 40.

Legay S, Guerriero G, André C, Guignard C, Cocco E, Charton S, Boutry M, Rowland O, Hausman J. 2016. MdMYB93 is a regulator of suberin deposition in russeted apple fruit skins. *New Phytologist*, **212**, 977–991.

Li J, Qin R, Fang Y, Gao Y, Jiao Y, Wei J, Bai S, Ni J, Teng, Y. 2024. PpMYB114 partially depends on PpMYB10 for the promotion of anthocyanin accumulation in pear. *Journal of Integrative Agriculture*, **24**, 4630–4642.

Li P M, Zhang Y Z, Einhorn T C, Cheng L L. 2014. Comparison of phenolic metabolism and primary metabolism between green 'Anjou' pear and its bud mutation, red 'Anjou'. *Physiologla Plantarum*, **150**, 339–354.

Li T, Jiang Z Y, Zhang L C, Tan D M, Wei Y, Yuan H, Li T L, Wang A D. 2016. Apple (*Malus domestica*) MdERF2 negatively affects ethylene biosynthesis during fruit ripening by suppressing MdACS1 transcription. *Plant Journal*, **88**, 735–748.

Liu T J, Zhang Y Z, Zhang X H, Sun Y Y, Wang H P , Song J P, Li X X. 2019a. Transcriptome analyses reveal key genes involved in skin color changes of 'Xinlimei' radish taproot. *Plant Physiology and Biochemistry*, **139**, 528–539.

Liu W, Wei Y, Sha S, Xu Y, Li H, Yuan H, Wang A. 2023. The mechanisms underpinning anthocyanin accumulation in a red-skinned bud sport in pear (*Pyrus ussuriensis*). *Plant Cell*

Reports, **42**, 1089–1105.
Liu Y F, Qi Y W, Zhang A L, Wu H X, Liu Z D, Ren X L. 2019b. Molecular cloning and functional characterization of AcGST1, an anthocyanin-related glutathione S-transferase gene in kiwifruit (*Actinidia chinensis*). *Plant Molecular Biology*, **100**, 451–465.
Luo H F, Dai C, Li Y P, Feng J, Liu Z C, Kang C Y. 2018. *Reduced Anthocyanins in Petioles* codes for a GST anthocyanin transporter that is essential for the foliage and fruit coloration in strawberry. *Journal of Experimental Botany*, **69**, 2595–2608.
Ni J B, Premathilake A T, Gao Y H, Yu W J, Tao R Y, Teng Y W, Bai S L. 2021. Ethylene-activated PpERF105 induces the expression of the repressor-type R2R3-MYB gene *PpMYB140* to inhibit anthocyanin biosynthesis in red pear fruit. *Plant Journal*, **105**, 167–181.
Premathilake A T, Ni J, Bai S, Tao R, Teng Y. 2020. R2R3-MYB transcription factor PpMYB17 positively regulates favonoid biosynthesis in pear fruit. *Planta*, **252**, 59.
Shao D, Li Y, Zhu Q, Zhang X, Liu F, Xue F, Sun J. 2021. *GhGSTF12*, a glutathione S-transferase gene, is essential for anthocyanin accumulation in cotton (*Gossypium hirsutum* L.). *Plant Science*, **305**, 110827.
Sun Y, Li H, Huang J R. 2012 Arabidopsis TT19 functions as a carrier to transport anthocyanin from the cytosol to tonoplasts. *Molecular Plant*, **5**, 387–400.
Teng S, Keurentjes J, Bentsink L, Koornneef M, Smeekens S. 2005. Sucrose-specific induction of anthocyanin biosynthesis in Arabidopsis requires the *MYB75/PAP1* gene. *Plant Physiology*, **139**, 1840–1852.
Wang L, Bolitho K, Grafton K, Kortstee A, Karunairetnam S, McGhie T K, Espley R, Hellens R P, Allan A C. 2010. An R2R3 MYB transcription factor associated with regulation of the anthocyanin biosynthetic pathway in Rosaceae. *BMC Plant Biology*, **10,** 50.
Wang X Q, Cao X Y, Shang Y, Bu H D, Wang T Y, Lyu D G, Du G D. 2020. Preharvest application of prohydrojasmon affects color development, phenolic metabolism, and pigment-related gene expression in red pear (*Pyrus ussuriensis*). *Journal of the Science of Food and Agriculture*, **100**, 4766–4775.
Wang X Q, Li C Y, Liang D, Zou Y J, Li P M, Ma F W. 2015. Phenolic compounds and antioxidant activity in red-fleshed apples. *Journal of Functional Foods*, **18**, 1086–1094.
Wang X Q, Liu S Q, Sun H L, Liu C Y, Li X Y, Liu Y, Lyu D G, Du G D. 2021. Production of reactive oxygen species by *PuRBOHF* is critical for stone cell development in pear fruit. *Horticulture Research*, **8**, 249.
Xu W, Dubos C, Lepiniec L. 2015. Transcriptional control of flavonoid biosynthesis by MYB–bHLH–WDR complexes. *Trends in Plant Science*, **20**, 176–185.
Yang Y N, Zhao G, Yue W Q, Zhang S L, Gu C, Wu J. 2013. Molecular cloning and gene expression differences of the anthocyanin biosynthesis-related genes in the red/green skin color mutant of pear (*Pyrus communis* L.). *Tree Genet Genomes***, 9**, 1351–1360.
Yao G F, Ming M L, Allan A C, Gu C, Li L T, Wu X, Wang R Z, Chang Y Z, Qi K J, Zhang S L, Wu J. 2017. Map-based cloning of the pear gene *MYB114* identifies an interaction with other transcription factors to coordinately regulate fruit anthocyanin biosynthesis. *Plant Journal*, **92**, 437–451.
Young M D, Wakefield M J, Smyth G K, Oshlack A. 2010. Gene ontology analysis for RNA-seq: Accounting for selection bias. *Genome Biology*, **11**, R14.
Zhai R, Wang Z M, Zhang S W, Meng G, Song L Y, Wang Z G, Li P M, Ma F W, Xu L F. 2016. Two MYB transcription factors regulate flavonoid biosynthesis in pear fruit (*Pyrus bretschneideri* Rehd.). *Journal of Experimental Botany*, **67**, 1275–1284.
Zhang Z, Tian C P, Zhang Y, Li C Z Y, Li X, Yu Q, Wang S, Wang X Y, Chen X S, Feng S Q. 2020. Transcriptomic and metabolomic analysis provides insights into anthocyanin and procyanidin accumulation in pear. *BMC Plant Biology*, **20**, 129.
Zhao J, Dixon R A. 2010. The 'ins' and 'outs' of flavonoid transport. *Trends in Plant Science*, **15**, 72–80.
Zhao Y, Dong W Q, Zhu Y C, Allan A C, Wang K, Xu C J. 2020. *PpGST1*, an anthocyanin-related glutathione S-transferase gene, is essential for fruit coloration in peach. *Plant Biotechnology Journal*, **18**, 1284–1295.
Zhao Y W, Wang C K., Huang X Y, Hu D G. 2021. Genome-wide analysis of the glutathione S-transferase (GST) genes and functional identification of *MdGSTU12* reveals the involvement in the regulation of anthocyanin accumulation in apple. *Genes*, **12**, 1733.

Executive Editor-in-Chief Sanwen Huang
Managing Editor Lingyun Weng